Modelling and simulation of condensation phenomena of acid gases in an industrial chimney

Eric Serris, Michel Cournil, Jérôme Peultier

XI° Congrès de la Société Française de Génie des Procédés. Des réponses industrielles pour une société en mutation. Saint Etienne, 9 au 11 octobre 2007, N°96, 2-910239-70-5

Modelling and simulation of condensation phenomena of acid gases in an industrial chimney

SERRIS Eric [a], COURNIL Michel [b*], PEULTIER Jérôme [c]

[a] *ENSM-SE, Centre SPIN, Département ProcESS, LPMG (UMR CNRS 5148) 158, Cours Fauriel, 42023 Saint-Etienne Cedex 02*
[b] *ENSM-SE, Centre SPIN, Département GENERIC, LPMG (UMR CNRS 5148) 158, Cours Fauriel, 42023 Saint-Etienne Cedex 02*
[c] *INDUSTEEL, CRMC, Arcelor Group, 56, rue Clemenceau, BP 19, 71201 Le Creusot Cedex, France*

Abstract

Coal power stations as well as waste incinerators produce humid acid gases which condensate in industrial chimneys. These condensates may cause corrosion of the internal cladding made of stainless steels, nickel base alloys or non metallic materials. In the aim of polluting emission reduction and material optimal choice, it is necessary to determine all the phenomena which occur throughout the chimney such as condensation and dissolution of acid gases (in this particular case, sulphur dioxide SO_2).
The production of energy from fossil fuels (coal, petroleum, natural gas, etc.) brings about the emission of gas containing sulphur compounds (SO_2, SO_3) as well as chlorine and fluorine compounds. To avoid this atmospheric pollution and its harmful effects (acid rains, impact on the health) due to hydrochloric, sulphuric and hydrofluoric acids produced in the presence of air, it is necessary to steam these flue gases. Nevertheless, a considerable quantity of residual acid gases remains in the gas discharge which also contains large amounts of water vapour.
Thus, condensation may occur and by the way an acid attack of the internal cladding of the chimney. This results in high costs of maintenance and a reduction of their structural stability. The knowledge of the phenomena of heat and mass transfer during the condensation of these acid gases in chimney is essential for their conception and materials choice.

Keywords:

modelling ; polluting emission ; mass and heat transfer ; industrial chimney ; acid gases

1. Modelling

In this modelling part of our work, we determine at first heat transfers in and around the chimney taking into account the condensation phenomenon. Then, we bring in the dissolution of one acid gas (SO_2) in the condensed phase. Modelling was performed in steady state conditions. The elements of this modelling are represented in Figure 1.

We adopt a simplified description for the temperature distribution, that is to say, T_g, gas temperature in on the chimney axis, T_{wi} temperature on the internal wall and T_{we} on the external wall while T_{ext} is the outside temperature. R is the chimney radius, L its total height and e the thickness of the wall.

We consider condensation of water vapour along the wall in the shape of a film. We call v the average drainage velocity of the water film, δ its thickness and T_d the surface temperature of this flowing film. T_d corresponds to the condensation temperature of the water vapour at local

* Corresponding Author: cournil@emse.fr

conditions of the chimney. This hypothesis was already applied by Nusselt in the first models (Nusselt, 1916).

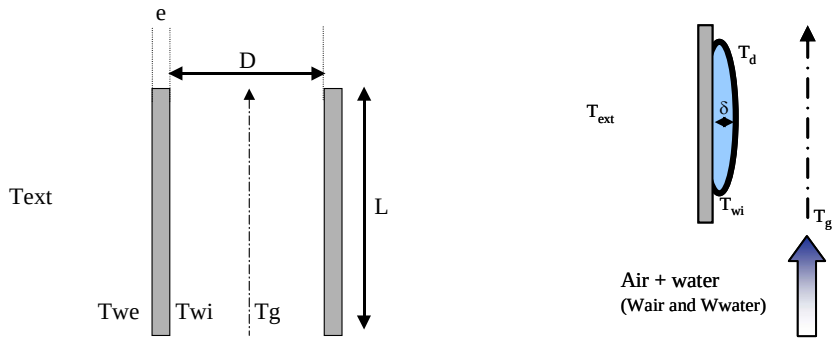

Figure 1. Chimney with and without condensation

To establish the equations describing the overall phenomena, mass and heat balance are written on a slice of chimney of thickness dz. All the obtained equations are listed below:

$$\frac{dW_{water}}{dz} = \frac{-2W_{cond}}{R} = \frac{-2H(T_{wi} - T_{ext}) + h_{int}(T_g - T_d)}{R}$$ Mass balance of water vapour (1)

$$\frac{dT_g}{dz} = \frac{-h_{int}(T_g - T_d)}{R(Cp_{water}W_{water} + Cp_{air}W_{air})}$$ Heat balance (2)

$$\delta(z) = \sqrt[3]{\frac{3R\mu_{water}(W_{water}(z) - W_{water}(0))}{2\rho_{water}^2 g}}$$ Global mass balance of water (3)

$$v = \frac{\rho_{water} g \delta^2}{3\mu_{water}}$$ Flow of the liquid film of condensate water (Beschkov *et al.*, 1978) (4)

$$T_{wi} = \left(\frac{1}{1 + \frac{\delta * H}{K_{water}}}\right)T_d + \left(H + \frac{\delta}{H\delta + K_{water}}\right)T_{ext}$$ Continuity of heat flow (5)

W_{water}, W_{air} and W_{cond} are respectively the mass flow rate of water, air and condensation, C_{pair} and Cp_{water}, the calorific capacities of air and water, μ_{water} the fluid dynamic viscosity (water), K_{water} is the water thermal conductivity and H the coefficient of global heat transfer defined by the following relation:

$\frac{1}{H} = \frac{1}{h_{ext}} + \frac{e}{k}$ with *k* the wall heat conductivity. To solve these equations it is necessary to know the heat transfer coefficients h_{int} and h_{ext} respectively inside and outside the chimney. To determine h_{ext}, we use a usual correlation for perpendicular flow (wind) to the axis of the chimney (Žukauskas and Žingžda, 1986)

$$Nu = 0.023 \mathrm{Re}^{4/5} \mathrm{Pr}^{2/5} = \frac{h_{ext}(D + 2e)}{k}$$

Here comes the following expression for h_{ext}:

$$h_{ext} = 0.023\frac{k(T_{ext})}{(D+2e)}\mathrm{Re}^{4/5}\,\mathrm{Pr}^{2/5} = 0.023\frac{k(T_{ext})}{(D+2e)}\left(\frac{v_{wind}*(D+2e)}{\nu(T_{ext})}\right)^{4/5}\left(\frac{\nu(T_{ext})}{\alpha(T_{ext})}\right)^{2/5}$$

v_{wind} is wind velocity outside the chimney.

For a tubular turbulent flow inside the chimney with a Reynolds number quite high ($Re > 10^4$) the following correlation is reliable (Mac Adams, 1942):

$$Nu = 0.023\,\mathrm{Re}^{4/5}\,\mathrm{Pr}^{1/3} = \frac{h_{int}D}{k}$$

We choose the following expression for h_{int}:

$$h_{int} = 0.023\frac{k(T_g)}{D}\mathrm{Re}^{4/5}\,\mathrm{Pr}^{1/3} = 0.023\frac{k(T_g)}{D}\left(\frac{4*W_{air}*D}{\pi*D^2*\nu(T_g)}\right)^{4/5}\left(\frac{\nu(T_g)}{\alpha(T_g)}\right)^{1/3}$$

With k(T) heat conductivity of gases inside the chimney, ν(T) kinematic viscosity and α(T) thermal diffusivity.

The reaction of absorption of sulphur dioxide gas into water is as follows:

$$H_2O + SO_2 \rightarrow H_2SO_3 \qquad K(T) = \frac{[H_2SO_3]}{P_{SO_2}}$$

We can thus obtain the sulphurous acid concentration (H_2SO_3) as a function of the partial pressure of the sulphur dioxide (SO_2) and the solubility constant K (T). This constant is deduced from the literature data (Hackspill *et al.*, 1964) and its expression is $K(T_{eq})$ = 7.18 exp-(0.0341*T_{eq}). We can also replace the sulphurous acid concentration to obtain the pH as a function of temperature and sulphur dioxide partial pressure:

$$pH = -\log\left(\frac{-K_{a1}+\sqrt{K_{a1}^2+4K_{a1}Ca}}{2}\right) = -\log\left(\frac{-K_{a1}+\sqrt{K_{a1}^2+4K_{a1}*7.18\exp(-0.0341Teq)P_{SO_2}}}{2}\right)$$

All these equations are now coded in a program using Matlab and solutions of the corresponding differential equations are obtained thanks to the internal solvers of the program.

2. Examples of model application

We are now going to apply the models previously obtained on two real cases of chimney: waste incinerators on one hand and coal power station on the other hand.

2.1 Coal power station

First, let us remind the chimney parameters as well as the operating conditions of this station: W_{air} = 2606310 m³/h or 2634247 kg/h, W_{water} = 144290 kg/h (i.e. 5.48%), D = 6.8 m (or 3.8m), gas temperature incoming at the lowest part of the chimney (z = 0) is T_{gas} = 89 °C (or 109°C maximal), v_{gas} = 34 m.s^{-1}. We admit that external temperature is T_{ext}= 25°C and wind velocity 10 m.s^{-1}. In this case our model predicts condensation of water at 9500 meters height, which is far from the real height of the chimney (L = 225 m)!

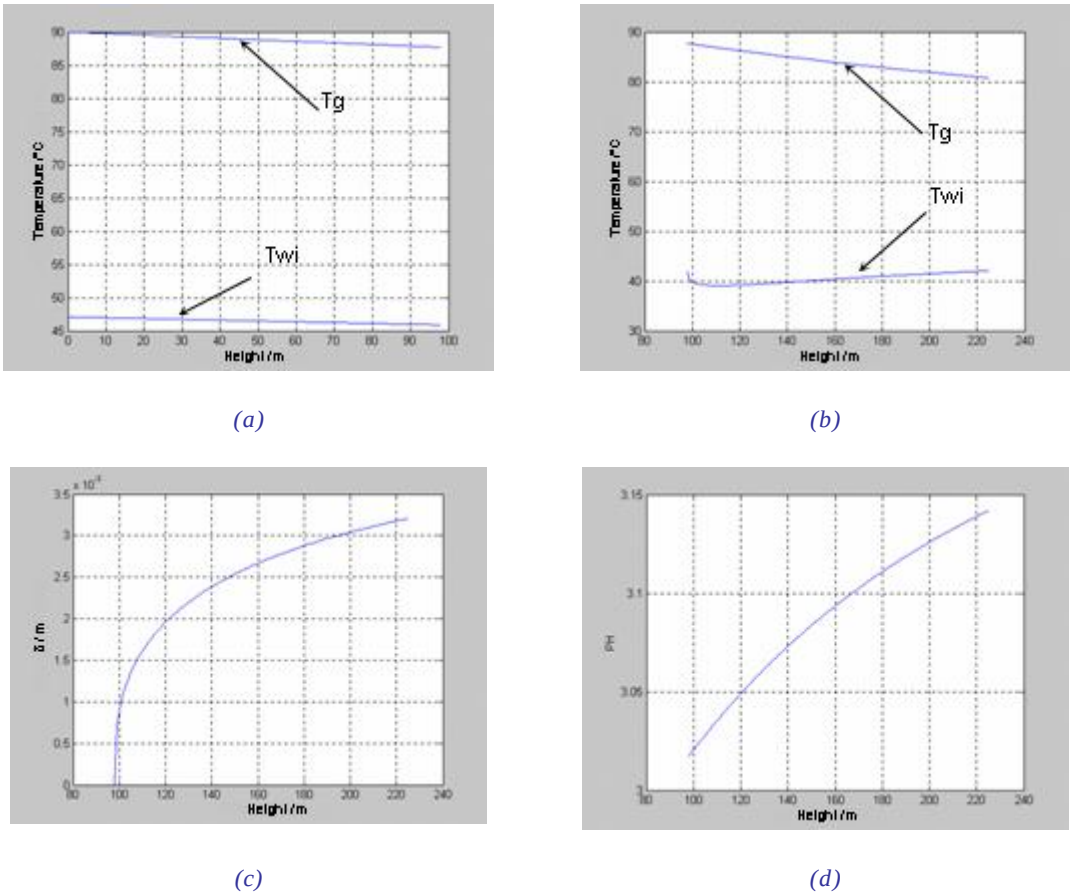

Figure 2. variation of gas temperature of the wall before (a) and after (b) condensation and thickness of the liquid film (c) and its pH (d) versus the height in the chimney

To obtain a condensation which occurs inside the chimney it is necessary to have different external conditions and also a water flow rate a little higher. These conditions are for instance water flow rate corresponding to 10 % of overall flow rate, wind velocity outside the chimney equal to 22m.s^{-1} and outside temperature of 0°C. The results obtained in this case are shown below. The first two graphs are the temperatures of the gas and the internal wall before (a) and after (b) condensation as a function of the height in the chimney. Two other graphs are the thickness of the flowing film (c) and the pH (d) (considering only the dissolution of sulphur dioxide) as a function of the height in the chimney.

The flowing film of condensate water is forming at approximately 100 meters. We can notice that the temperature of the gas at the top of the chimney does not drop much with regard to the initial temperature. Furthermore, we notice that the thickness of the flowing film is some millimeters thick and that the pH is rather low (pH ~3) and does not vary a lot.

2.2 Waste incinerators

First, here are the parameters of the chimney as well as the operating conditions of this incinerator: W_{air} = 173400 m^3/h; W_{water} = 31212 m^3/h (18% of total flow, can rise up to 25%); L = 100 m ; D = 2.2 m ; T_{gas} = 67°C (or 100°C maximal)

For an outside temperature of 25°C and a wind of velocity 10m.s^{-1}, we obtain the following results. Figure 3(a) represents the evolution of gas temperatures (the most important parameter) and wall temperature versus height in the chimney (in meters). Figure 3(b) shows the thickness of the water film (in meters) versus the height (in meters), Figure 3(c) the pH versus the height in the chimney.

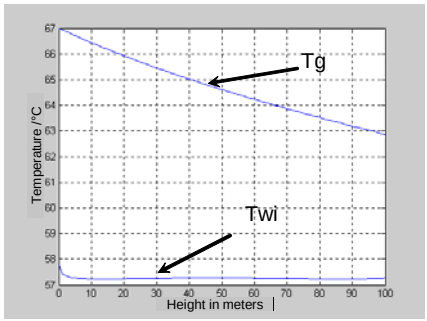

(a)

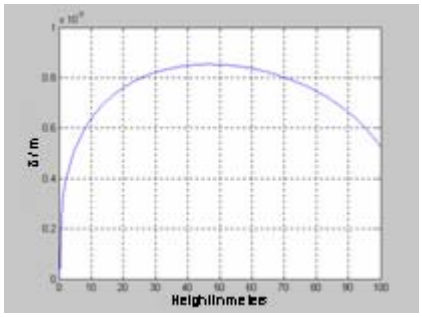

(b)

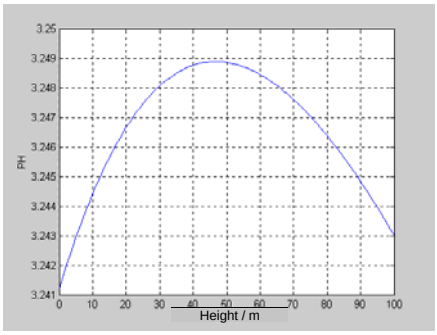

(c)

Figure 3. Variation of gas and wall temperature (a) liquid film thickness (b) and its pH (c) versus the height in the chimney

In this example, we observe a liquid film flowing on the whole the height of the chimney. We observe again moderate variations of the different temperatures. The flowing film is a few millimetres thick and the calculated pH (again about 3) is almost constant. Condensation does not take place on all the height of the chimney for lower wind speed outside (because then the external transfer coefficient becomes sharply lower). For example an outside wind of 2m.s^{-1} leads to condensation after 60 m.

These results derived from our modelling are quite interesting because they prove that corrosion may be found only from a certain height and not on the entire chimney. Indeed, the film does not flow sometimes on the totality of the chimney. Only a part of the chimney requires then a steel cladding resisting to the corrosion, for the rest of a less noble and cheaper material should be sufficient.

3. Experiments

The purpose of these experiments is not to perform a pilot plan of a chimney but rather to understand different phenomena which take place during the condensation. This should allow us to confirm or not the hypotheses taken in the model.

3.1 Experimental set-up

We tried to build a set-up which could allow us to observe water condensation in a long tube for various experimental conditions. Its schematic representation is shown in Figure 4.

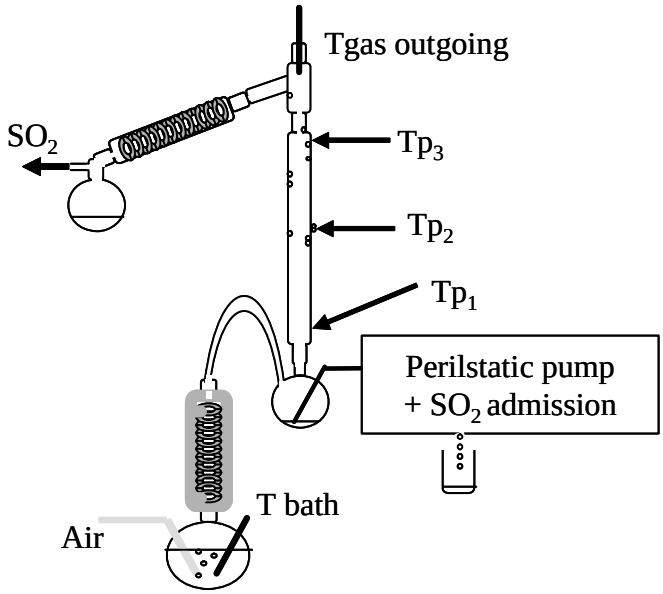

Figure 4. Experimental set-up

A three neck flask of water with fixed temperature with air flow bubbling, allows us to ensure relative humidity corresponding to the industrial conditions. The wet gas produced is preheated in a tube surrounded with heating cords and then pumped into another three neck flask also surrounded with heating cords. A long glass tube acts like the industrial chimney by allowing the condensation of water but also a qualitative and quantitative observation of condensation and flowing film. At the top of the set-up, the gas is passed to a cooling tube so that the rest of water vapour condensates. A thermometer is placed in this part to measure the gas temperature which goes out of the column. We indicated in Figure 4 three points of measure (T_{p1}, T_{p2} and T_{p3}) of the wall temperature. After flowing along the tube, water is pumped up by a peristaltic pump and collected in a beaker. Non condensed vapour is collected too at the top of the column. From the ratio of these two samples of water, we obtain the percentage of condensed water (noted %E.R).

3.2 Influence of gas humidity

We vary now the temperature of the flask in order to have a variation of water content (or moisture content) in the gas from 10 to 20 % at gas flow of 300 NL.h^{-1}. Initial input gas temperature is 65°C up to 90°C. Figure 5 shows the variation of the temperature of the outgoing gas, the wall temperature at the bottom of the tube *T*p1 and of the ratio %E.R. versus the temperature of the entering gas.

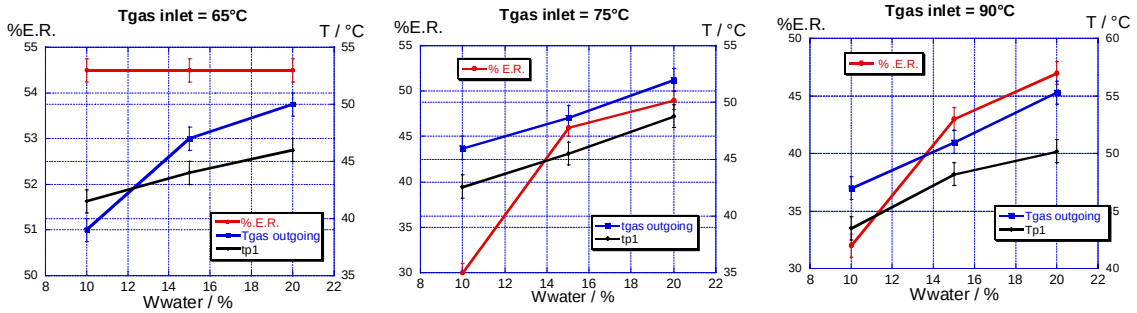

Figure 5. Influence of gas humidity

In each example, the wall temperature increases when the moisture content increases. It is qualitatively consistent with Equation (5) which gives the wall temperature as a function of film temperature T_d and external temperature T_{ext}:

$$T_{wi} = \left(\frac{1}{1+\frac{\delta * H}{K_{water}}}\right)T_d + \left(H + \frac{\delta}{H\delta + K_{water}}\right)T_{ext}$$

Temperature T_{wi} is thus increasing as a function of temperature T_d which corresponds (in this example) to the temperature of the flask which generates the water vapour. When this temperature increases it has the effect of increasing the internal wall temperature and thus the external wall as well as W_{water}. This is a consequence of the increasing variation of temperature T_{p1} according to W_{water}.

We also note a constant increase of T_g with W_{water}. If we come back to formula (2) which describes the evolution of T_g:

$$\frac{dT_g}{dz} = \frac{-h_{int}(T_g - T_d)}{R(C_{p_{water}}W_{water} + Cp_{air}W_{air})}$$

We also notice that an increase in T_d (or equivalently W_{water}) causes the decrease of the absolute value of the derivative function of T_g versus z. As a consequence, the outgoing gas temperature of the chimney increases.

We also observe an increase of %E.R versus increasing W_{water} excepted for the lowest gas temperature. Equation (1) gives the expression of W_{cond}:

$$W_{cond} = \frac{q_{ext} - q_{int}}{\Delta H_{cond}} = \frac{H(T_{wi} - T_{ext}) - h_{int}(T_g - T_d)}{\Delta H_{cond}}$$

When T_d increases, q_{int} decreases and W_{cond} increases what is observed indeed in Figure 5.

There is however a problem to explain the results obtained for gas temperature of 65°C. In these conditions, we note that % .E.R is constant and thus W_{water} has no influence on the condensation. At the moment we have no clear explanation of the phenomenon.

3.3 Influence of SO_2

The sulphur dioxide is not introduced at first. Experiment begins as previously in order to have condensation of water on the tube walls. Then sulphur dioxide is introduced (200 ppm of SO_2 dilute in air) as shown in Figure 4. Experiments involving SO_2 are 90 min long.
Condensed water which is recovered at the top and the bottom of the column can be then characterized. Ionic chromatography in a DIONEX apparatus is used as main analysis technique.
An example of chromatogram of both solutions collected at the top and at the bottom of column is presented in Figure 6.

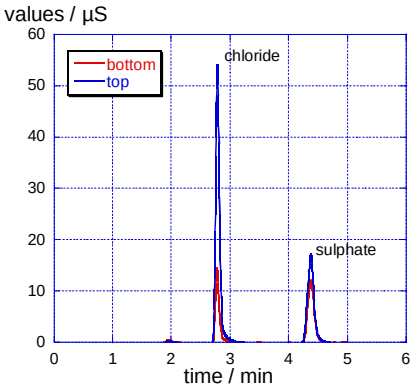

Figure 6. Water condensate collected chromatograms

The presence of chlorides on chromatograms is simply due to pollution of beakers. It should not be taken into account. We can determine the concentration in sulphate ion thanks to standardization performed with solutions of known concentrations. For example, three different experiments results are shown in the following table.

Table 1. Concentrations top and bottom

n° exp	parameters		m water (g)	$[SO_4^{2-}]$ chromato	pH	$[SO_4^{2-}]$ pH
1	300 NL.h-1; T_{gas} = 75 °C, 200 ppm SO_2 10 % water	top	10.2	15.6 $g.L^{-1}$	3.55	13.5 $g.L^{-1}$
		bottom	14.8	13.0 $g.L^{-1}$	3.55	13.5 $g.L^{-1}$
2	300 NL.h-1; T_{gas} = 75 °C, 200 ppm SO_2 10 % water	top	12.0	14.5 $g.L^{-1}$	3.52	14.5 $g.L^{-1}$
		bottom	18.6	10.2 $g.L^{-1}$	3.73	8.9 $g.L^{-1}$
3	300 NL.h-1; T_{gas} = 105 °C, 200 ppm SO_2 10 % water	top	14.0	5.6 $g.L^{-1}$	4	4.8 $g.L^{-1}$
		bottom	9.8	10.9 $g.L^{-1}$	3.73	8.9 $g.L^{-1}$

Experiments 1 and 2 are intended to test the reproducibility of our experiments. This reproducibility is quite good, given that we do not control the quantity of condensed water in the flowing film on the walls before the introduction of SO_2. Indeed, we note the same quantity of water at the top and at the bottom of the column with similar pH and concentration in sulphate ions.

If we compare now experiments 2 and 3, only the temperature of the entering gas is modified. We recover less water at the bottom of the chimney thus we have less condensation as we observed in the first experiences. Furthermore, the concentrations in sulphate at the bottom of the column for both experiments are the same, even if we obtain in a case twice more water. This is due to the fact that the absorption of SO_2 depends on the temperature of the water condensed on the walls. This temperature is fixed by the temperature of the lower three neck flask which does not change in both experiments.

4. Conclusion

The model we developed reveals a fair consistency with the experimental observations. These observations, however, give us interesting tracks to refine the model. In the absence of a pilot, the laboratory column allowed us to validate the influence of the parameters such as input gas temperature, gas flow rate as well as percentage of water in gas. However as well in the reality as in the model, the most important parameters are in fact internal and external heat coefficients transfers which govern the main thermal processes. External heat coefficient is above all determined by the weather conditions thus it is hardly controllable and can be considered as imposed. As for the internal heat coefficient, it is very sensitive regarding internal gas velocity, and correlations which allow its calculation have a questionable reliability. An experimental identification on installation or on pilot plan should be imperative. Concerning pH of the flowing film of condensate water, last experiments shows that the dissolution of the SO_2 is rather fast and the flowing film acidity is quite high even in presence of a small amount of SO_2. A dynamic modelling could be envisaged but should be more complex because, for instance, it should involve friction coefficient (kinematic or dynamic) of the wall and also the wetting angle between wall and condensate. It also should take into account nucleation and breakage of the liquid film as well as all transfer kinetics which are often poorly understood processes. In spite of its simplicity, present study offers nevertheless an interest to predict qualitatively and

quantitatively the main phenomena (condensation) and the essential characteristics (zone of condensation, pH) of the industrial installations.

References

Beschkov, V. ; Boyadjiev, C. ; Peev, G.; 1978. On the mass transfer into a falling laminar film with dissolution. Chemical Engineering Science 33(1), 65-69

Hackspill L., Besson J., Herold A., 1964. Chimie Générale. Paris, Presses Universitaires de France, 416

Mac Adams, W., 1942. Heat transmission 2nd Edition, New-York, Mac Graw Hill, 168

Nusselt, W., 1916. Die Oberflächenkondensation des Wasserdampfes. VDI-Z. 60, 541-546, 569-575

Žukauskas, A.; Žingžda, J., 1986. Heat transfert of a cylinder in cross flow. Washington, Hemisphere Publications Company, 162